

Transverse Optical Mode in a One-Dimensional Yukawa Chain

Bin Liu,* K. Avinash, and J. Goree†

Department of Physics and Astronomy, The University of Iowa, Iowa City, Iowa 52242, USA
(Received 27 May 2003; revised manuscript received 11 September 2003; published 19 December 2003)

A transverse optical mode was observed in a one-dimensional Yukawa chain. Charged particles, suspended in a strongly coupled dusty plasma, were arranged in a 1D periodic structure. Particle displacement in the direction perpendicular to the chain was restored by the confining potential. The dispersion relation of phonons was measured, verifying that the optical mode has negative dispersion, with phase and group velocities that are oppositely directed. A theoretical dispersion relation is presented and compared to the experiment and a molecular dynamics simulation.

DOI: 10.1103/PhysRevLett.91.255003

PACS numbers: 52.27.Lw, 52.27.Gr, 82.70.Dd

A linear chain is a simple form of condensed state matter with a low dimensionality. Charged macroscopic-sized particles, levitated in a dusty plasma, can be confined in a single row, forming a 1D plasma crystal [1]. Colloidal particles, suspended in an aqueous solution, can be trapped in a potential well provided by two counter-propagating laser beam to form a 1D coupled array [2]. A 1D Coulomb chain confined in a storage ring [3] may be used in atomic clocks [4] or quantum computing [5]. At the atomic scale, a 1D chain can be found in compounds such as $\text{Hg}_{3-\delta}\text{AsF}_6$ [6], as well as low-dimensional systems formed on surfaces, such as chains of Au on Si(111) [7]. A 1D chain of gas atoms adsorbed in carbon nanotubes has been produced experimentally, and its phonon frequencies have been predicted theoretically assuming a Lennard-Jones potential [8,9].

Here we study a linear chain of charged particles that interact with a Yukawa potential, i.e., a shielded Coulomb repulsion. To study the chain experimentally, we use a dusty plasma consisting of electrons, ions, neutral atoms, and small particles of solid matter. The particles acquire a negative charge and are confined in an external potential. Because of mutual repulsion and external confinement, the particles can arrange themselves in a 1D structure. In 2D and 3D experiments, studies have included the melting transition [10,11] and phonon propagation [12–14].

An externally confined chain can vibrate with two modes. In the longitudinal mode [1], particle motions are compressional along the chain. In the other mode [15–17], particles move transverse to the chain, and their displacements are restored by an external confining potential; this is different from the transverse acoustic mode in a 2D lattice [12], where an in-plane restoring force is provided by interparticle interactions.

When the particles are mutually repulsive, we term this wave as the “transverse optical mode.” The word “optical” here does not refer to high-frequency electromagnetic waves. Instead, it is chosen in analogy with the optical mode in ionic crystals. In an extreme case of an ionic crystal, massive positive ions act as a “steady-state” ion matrix (in analogy with the confining potential for a

1D chain), and negative ions oscillate in the matrix. For the optical mode in an ionic crystal, the frequency decreases with wave number k , but does not extend down to zero frequency. It has a maximum frequency at $k = 0$ corresponding to a sloshing motion, with like ions all moving together.

We used the experimental setup sketched in Fig. 1(a). A plasma was produced in a capacitively coupled rf

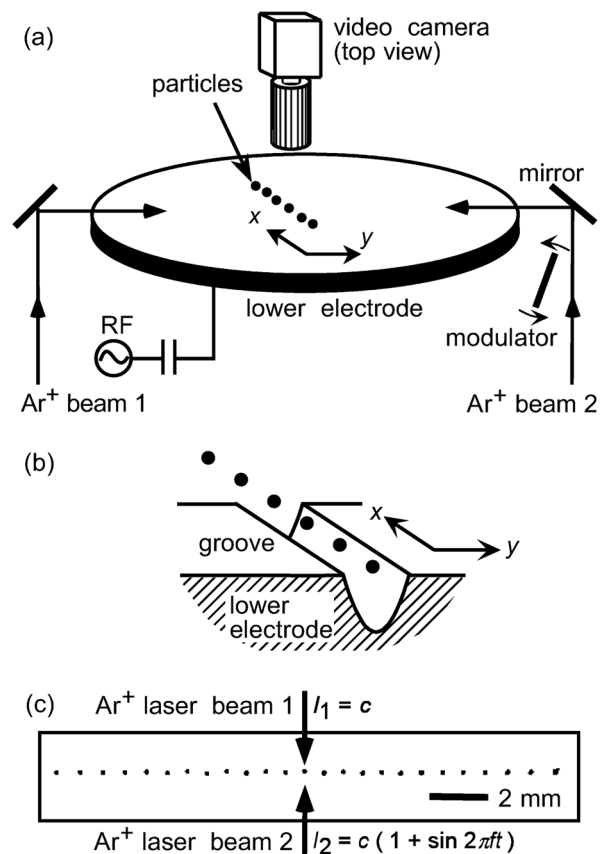


FIG. 1. (a) Apparatus. (b) Particles, levitated above a groove in the lower electrode, arrange themselves into a 1D chain. (c) Image of particles. At the chain’s center, two counter-propagating laser beams push a single particle in the y direction to excite a wave.

discharge, using a 13.56 MHz rf voltage with a peak-to-peak amplitude of 94 V and a self-bias of -48 V. A sheath formed immediately above the lower electrode. We used xenon gas at low pressure of ≈ 5 mtorr. The plasma had a density of $1.2 \times 10^9 \text{ cm}^{-3}$ and an electron temperature of 1.6 eV, as measured by a Langmuir probe located in the plasma glow region. We used a shaker to introduce a small number of particles with diameter of $8.09 \pm 0.18 \mu\text{m}$ and a mass density of 1.514 g/cm^3 . Particles were levitated in the sheath, well below the height of the Langmuir probe.

The interparticle potential consists of a shielded Coulomb interaction that is modified by a wakefield downstream of the particle. Konopka *et al.* [18] demonstrated that the binary interparticle potential for particles moving in a horizontal plane was accurately modeled by a simple Yukawa potential, over the range $0.77 < \kappa < 1.5$, where $\kappa = a/\lambda_D$, a is the interparticle distance, and λ_D is a shielding length.

We determined the particle's charge Q and λ_D using two methods. First, using a method based on particles' equilibrium position [19], we found that $\lambda_D = (0.86 \pm 0.07) \text{ mm}$ and less precisely $Q = (6476 \pm 1308)e$, where e is elementary charge. Second, constraining $\lambda_D = 0.86 \text{ mm}$, we found Q by fitting a dispersion relation of the longitudinal wave in the chain [1]. The final values were $\lambda_D = 0.86 \text{ mm}$ and $Q = 7595e$.

Particles were externally confined by natural electric fields in the sheath above the lower electrode. The sheath conforms to the shape of the electrode, which had a groove-shaped depression along the x direction, to form a 1D chain. Everywhere along the groove's length, it had a parabolic shape in the y direction [Fig. 1(b)] with a depth $z = y^2 - 4 \text{ mm}$ and a length of 80 mm. Figure 1(c) shows an image of the chain. The interparticle spacing was not uniform; it was 15% smaller in the center than at the chain's end.

We manipulated a single particle with two counter-propagating laser beams. Laser light exerts a radiation pressure on a particle, with a magnitude proportional to the laser intensity [20,21]. The intensity of one laser beam was modulated by a scanning mirror that periodically blocked a portion of the beam, yielding a sinusoidal intensity $I_2 = c[1 + \sin(2\pi ft)]$. The opposite laser had no modulation, $I_1 = c$, so that the net force applied to a particle was sinusoidal (Fig. 1).

We characterized the confinement by measuring the motion of a single particle, manipulated in the x or y direction using lasers and in the vertical direction by modulating the electrode voltage. The resonance frequencies of a single particle in the confining potential were 0.1, 3, and 15 Hz in the x , y , and vertical directions, respectively. The motion was harmonic in all three directions. The confinement in the vertical direction was strong enough to prevent any vertical buckling of the chain. By measuring the resonance curve for motion in the y direc-

tion, we determined the damping rate for a single particle $\nu_E = 3.5 \pm 0.3 \text{ s}^{-1}$. After these tests with a single particle, we introduced more particles to form a 1D chain. Using the vertical resonance method [11], we verified that Q was independent of the particle number N .

Waves were excited locally by manipulating a single particle near the chain's center using a sinusoidal force. Waves propagated away from that location. Because the particle was manipulated in the y direction, its motion coupled mostly into the transverse optical mode, although a longitudinal wave with an amplitude smaller by a factor of 10 was also excited. The wave amplitude was small to avoid nonlinearities.

One might expect that, in a 1D chain with a finite length, only standing waves would be allowed. However, we show in our experimental results that there was no significant reflected wave from the chain's end, due to gas damping.

To image the particles, we illuminated them with a HeNe laser sheet and viewed with a video camera at 29.97 frames per second. The field of view, $13 \times 10 \text{ mm}^2$, included only the central portion of the chain. Particle positions were measured in each frame with subpixel spatial resolution by intensity weighting, and particle velocities were calculated.

To measure the dispersion relation, we calculated the wave number $k = k_r + ik_i$ associated with each excitation frequency using a Fourier transformation of particles' velocities. The frequency ω is real because the wave was excited externally at a specific frequency. As the wave propagates, it is damped, so that k has an imaginary part. Calculating a wave's phase as a function of x (Fig. 2) and fitting to a straight line yields k_r . Similarly, fitting the amplitude to an exponential curve yields k_i .

Our chief experimental result is the dispersion relation of the transverse optical mode (Fig. 3). Results are shown

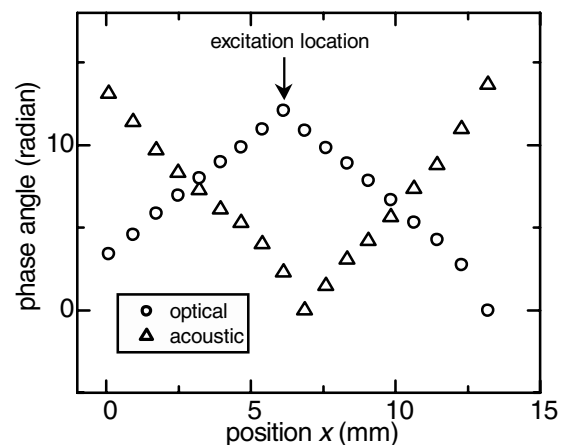


FIG. 2. Optical and longitudinal acoustic waves both propagated away from the excitation region. The phase dependence indicates they are backward and forward, respectively. Data are shown for $N = 28$.

for three different chain lengths, with $N = 10, 19,$ and 28 . For the central portion of the chain, where the wave was detected, $a = 1.2, 0.8,$ and 0.72 mm. These values were calculated from the first peak of the pair correlation function and correspond to $\kappa = 1.4, 1.0,$ and $0.84,$ respectively. The dispersion relations for both the transverse optical and longitudinal waves in Fig. 3 were prepared from the y and x components of particle velocities, respectively.

The dispersion relation depends on κ . For small κ , i.e., large N , the dispersion relation's curve is steeper, and damping is weaker. We note that for small κ the interparticle forces are larger.

We verified that, unlike the longitudinal mode, the transverse optical mode has a negative dispersion. The wave number decreases with an increasing of frequency, as seen in Fig. 3(a). The transverse optical mode is mostly constrained to a frequency band, between 11 and 21 s⁻¹ for $N = 28$. Similar results were reported in Ref. [17], in

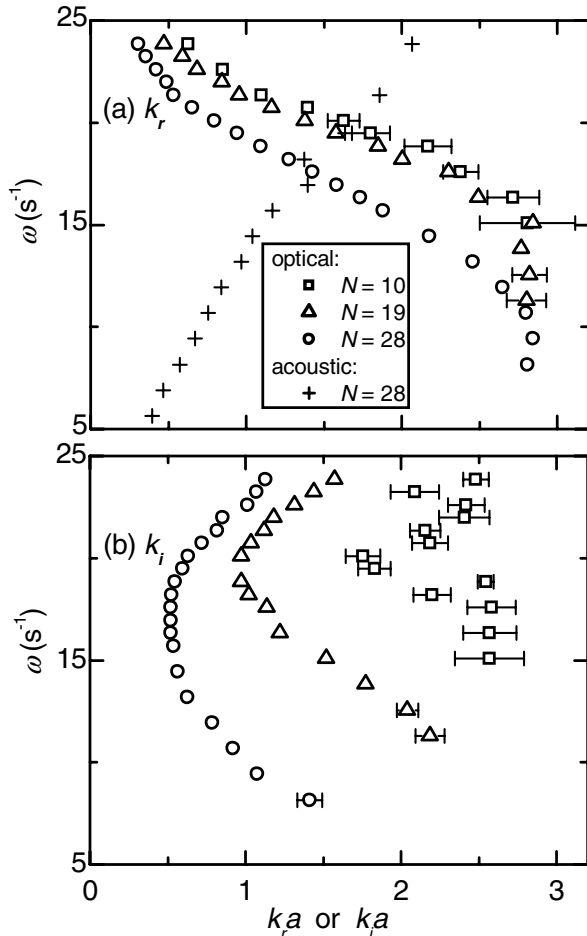


FIG. 3. Experimental dispersion relation. In the real part (a), ω decreases with k_r for the transverse optical wave. In the imaginary part (b), damping is smallest in a central frequency band. The dispersion relation depends on N because a and κ are smaller for larger N .

an experiment such as ours, except that the charge varied with time. We find that outside this band, the damping is larger.

Backward waves are characterized by phase and group velocities that are oppositely directed, and we see from Fig. 2 that this is so for the transverse optical mode. The group velocity is always directed away from the excitation region. For the transverse optical mode, the phase velocity is directed toward the excitation region, as indicated by a phase angle that decreases with distance from the excitation region. In contrast, the longitudinal wave has a phase angle that increases with distance, indicating that it is a forward mode.

Before reaching the chain's end, waves were mostly damped down to the level of the random motion, i.e., a rms velocity of 0.1 mm/s. Thus, any wave reflection at the chain's end will be insignificant.

A molecular dynamics simulation was performed using the experimental parameters. The particle's equation of motion was $m\ddot{\mathbf{r}}_i = -\nabla(\sum \phi_{ij} + \Phi_i^{\text{ext}}) - \nu_E m\dot{\mathbf{r}}_i + \mathbf{F}_L^y$, with a binary Yukawa interparticle interaction $\phi_{ij} = Q^2 e^{-r_{ij}/\lambda_D}/4\pi\epsilon_0 r_{ij}$, confining potential $\Phi_i^{\text{ext}} = m(\omega_x^2 x_i^2 + \omega_y^2 y_i^2)/2$, gas drag $\nu_E m\dot{\mathbf{r}}_i$, and laser radiation pressure force $F_L^y = f_0 \cos\omega t$. Here $\mathbf{r}_i = (x_i, y_i)$ is measured from the center of the chain, and r_{ij} is an interparticle distance. We chose the value of ω_x to yield the same interparticle distance as in the experiment, and for ω_y we used the experimental value. The amplitude f_0 of the laser radiation pressure force was chosen to yield the same wave amplitude, at the excitation location, as in the experiment. As in the experiment, we found a dispersion relation, shown with triangles in Fig. 4.

We also present a theoretical dispersion relation for linear wave in a chain at zero temperature. The theory has the same assumptions as in the simulation, except that it assumes the following: the chain is infinite in the x direction and has a uniform interparticle distance; the interparticle force is linearized with respect to distance; in converting the equation of motion to a wave equation and then a dispersion relation, it is not necessary to specify the source of energy as, for example, our laser radiation pressure; and the transverse mode does not couple with the longitudinal and vertical modes. This yields a dispersion relation for the transverse optical mode, having two equations that can be solved for k_r and k_i , for a specified real frequency ω :

$$\omega^2 = \omega_{\text{CM}}^2 - 2 \sum_{l=1}^{10} \omega_{0,l}^2 (1 + l\kappa) e^{-l\kappa} (1 - \cos lk_r a \cosh lk_i a),$$

$$\omega = 2 \sum_{l=1}^{10} \omega_{0,l}^2 \nu_E^{-1} (1 + l\kappa) e^{-l\kappa} \sin lk_r a \sinh lk_i a,$$

where $\omega_{0,l} = (Q^2/4\pi\epsilon_0 m a^3 l^3)^{1/2}$. We find that this dispersion relation depends significantly on the presence of damping, as discussed below.

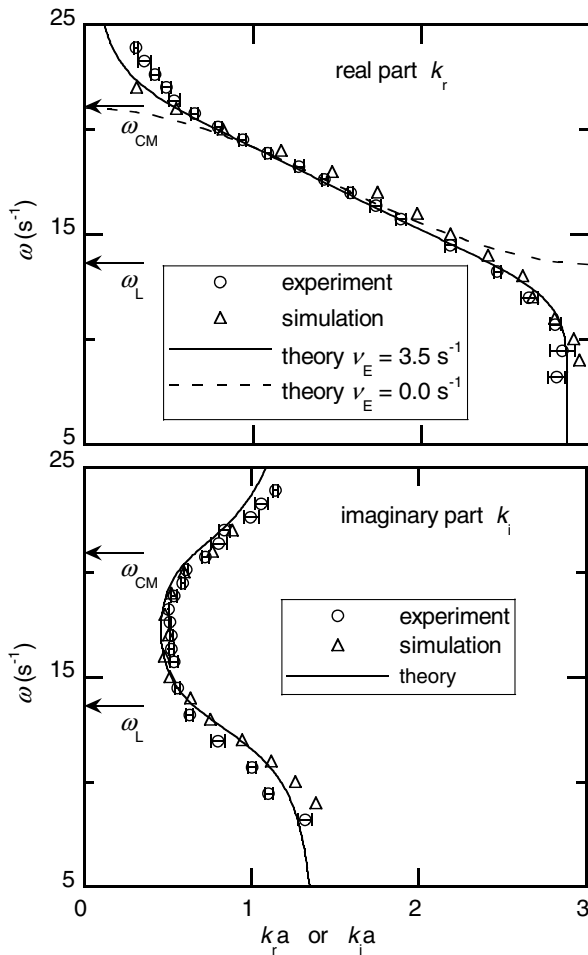


FIG. 4. Comparison of dispersion relations. In the experiment and simulation, $N = 28$. In the theory, $\kappa = 0.84$, the same as in the central portion of the chains in the experiment and simulation. In the absence of gas damping, the wave is evanescent outside the band $\omega_L < \omega < \omega_{CM}$.

In the absence of gas damping, this wave is allowed only in a frequency band between two cutoff frequencies, ω_L and ω_{CM} , as shown in Fig. 4 with $\nu_E = 0$. Outside this band the wave is evanescent, with an imaginary k . At $\omega = \omega_{CM}$, all particles move together, corresponding to the sloshing mode. At $\omega = \omega_L$, neighboring particles oscillate out of phase, corresponding to a standing wave.

With damping, the wave propagates beyond the frequency band that is allowed in the absence of damping. Outside this band, the wave is more heavily damped, and the real part has a steep slope.

Comparing the dispersion relations from theory and simulation (Fig. 4), we found that they agree, for both the real and imaginary parts. This agreement indicates that the assumptions of the theory that differ from the simulation (infinite chain with uniform spacing) do not profoundly affect the dispersion relation. They also agree with the experiment, so that we conclude the theory's assumptions are adequate; these include a Yukawa poten-

tial, parabolic confinement, uniform spacing, and the uncoupling of motions in y and z directions.

Finally, we discuss how the roles of the external confining potential and the repulsive interparticle potential cause the wave to be backward. The external confining force has a y component, and it restores a particle toward its equilibrium position at $y = 0$. When $k = 0$, all particles move together in a sloshing mode. When $k \neq 0$, neighboring particles have different values of y , so that their repulsive interparticle force vector has a y component that is oppositely directed to the restoring force. As a result, the net restoring force is reduced as k is increased. This weaker net force results in a slower oscillation, i.e., a smaller ω . Thus, ω decreases with k , and the wave is backward. If the interparticle force were not repulsive, the wave would not be backward [8,9].

We thank L. Boufendi for TEM measurements of particle size. We thank G. Kalman and F.M. Peeters for helpful discussions. This work was supported by NASA and DOE.

*Electronic address: bliu@newton.physics.uiowa.edu

†Electronic address: john-goree@uiowa.edu

- [1] A. Homann, A. Melzer, S. Peters, and A. Piel, Phys. Rev. E **56**, 7138 (1997).
- [2] S. A. Tatarikova, A. E. Carruthers, and K. Dholakia, Phys. Rev. Lett. **89**, 283901 (2002).
- [3] G. Birkel, S. Kassner, and H. Walther, Nature (London) **357**, 310 (1992).
- [4] W. M. Itano and N. F. Ramsey, Sci. Am. **269**, 56 (1993).
- [5] J. I. Cirac and P. Zoller, Phys. Rev. Lett. **74**, 4091 (1995).
- [6] I. D. Brown, Can. J. Chem. **52**, 791 (1974).
- [7] P. Segovia *et al.*, Nature (London) **402**, 504 (1999).
- [8] M. T. Cvitas and A. Siber, Phys. Rev. B **67**, 193401 (2003).
- [9] A. Siber, Phys. Rev. B **66**, 235414 (2002).
- [10] H. M. Thomas and G. E. Morfill, Nature (London) **379**, 806 (1996).
- [11] A. Melzer, A. Homann, and A. Piel, Phys. Rev. E **53**, 2757 (1996).
- [12] S. Nunomura, D. Samsonov, and J. Goree, Phys. Rev. Lett. **84**, 5141 (2000).
- [13] J. B. Pieper and J. Goree, Phys. Rev. Lett. **77**, 3137 (1996).
- [14] V. Nosenko, S. Nunomura, and J. Goree, Phys. Rev. Lett. **88**, 215002 (2002).
- [15] S. V. Vladimirov, P. V. Shevchenko, and N. F. Cramer, Phys. Rev. E **56**, R74 (1997).
- [16] A. V. Ivlev and G. E. Morfill, Phys. Rev. E **63**, 016409 (2000).
- [17] T. Misawa *et al.*, Phys. Rev. Lett. **86**, 1219 (2001).
- [18] U. Konopka, G. E. Morfill, and L. Ratke, Phys. Rev. Lett. **84**, 891 (2000).
- [19] B. Liu, K. Avinash, and J. Goree, Phys. Rev. E (to be published).
- [20] B. Liu, J. Goree, V. Nosenko, and L. Boufendi, Phys. Plasmas **10**, 9 (2003).
- [21] A. Ashkin, Phys. Rev. Lett. **24**, 156 (1970).